

# Identification of Sources of Methane in Ho Chi Minh City, Vietnam

Ceres A. Woolley Maisch,\* James L. France, Rebecca E. Fisher,\* David Lowry, Grant Forster, Thi Hien To, Itziar Irakulis-Loitxate, Nicholas Garrard, Doan Thien Chi Nguyen, Thi Thanh Nhon Nguyen, Hoang Minh Tran, Vo Tu Uyen Nguyen, Gia Luat Nguyen, Ha Phuc Duy Cao, Graham Mills, David Oram, Thomas Röckmann, Carina van der Veen, and Euan G. Nisbet



Cite This: *ACS EST Air* 2026, 3, 649–661



Read Online

ACCESS |



Metrics & More



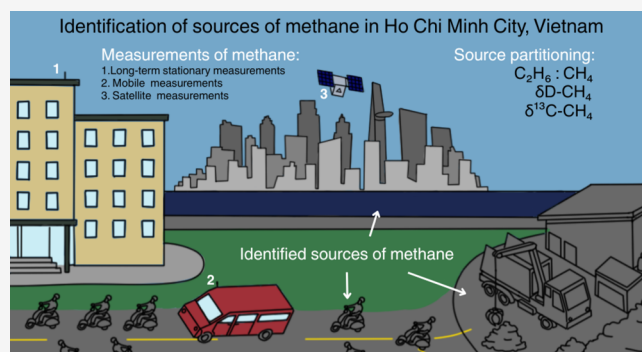
Article Recommendations



Supporting Information

**ABSTRACT:** Stationary, mobile, and satellite measurements of methane are evaluated to characterize and distinguish the major sources of methane emissions in Ho Chi Minh City, Vietnam. The isotopic composition of the methane and ethane:methane ratios resulted in the successful differentiation between source categories, and the results indicate that the main emission sources in the city are from waste and traffic. The most significant source of CH<sub>4</sub> was the Da Phuoc landfill site to the south of the city, which was responsible for elevated CH<sub>4</sub> mole fractions over large parts of the city; more than 1 ppm above background up to 15 km away. With this large extent and elevation, we show that during the study period, the landfill emissions are detectable from space using the PRISMA satellite. Our measurements in an understudied region offer an empirical basis to guide methane management and mitigation strategies implemented by governments to achieve the goals of the Global Methane Pledge.

**KEYWORDS:** methane, methane isotopologues, urban emissions, South East Asia



## INTRODUCTION

Methane is the second most important anthropogenic greenhouse gas in the atmosphere, it has a global warming potential of 27–30 over a 100-year time scale.<sup>1</sup> Methane's perturbation lifetime in the atmosphere is around 12 years.<sup>1</sup> This short lifetime means that the positive impact of mitigation (such as keeping the global average temperature below 2 °C warming compared to preindustrial levels) of methane emissions will occur at a much shorter time scale than that of CO<sub>2</sub>, the lifetime of which can be on the order of centuries. However, the current growth rates of CH<sub>4</sub> (which in 2024 was 8.62 ± 0.59 ppb, according to Lan et al.<sup>2</sup>) pose a threat to the success of the Paris climate agreement.<sup>3</sup> Therefore, the identification of sources of methane, so that the successful and efficient mitigation of these emissions can be targeted, is required.

Under the United Nations Framework Convention on Climate Change (UNFCCC), efforts have been made to improve the quantification of greenhouse gas emissions globally. In Vietnam, there is a justified focus on rice paddy methane emissions,<sup>4–8</sup> as well as some studies into methane emissions from landfills.<sup>9–11</sup> The urban methane emissions measured by mobile atmospheric surveys have never been reported at the street level in this country, as far as the

published literature suggests. Additionally to street level mobile measurements, this study includes long-term in situ measurements, isotopic analysis, and satellite observations. Mobile measurement methodologies have been tested and implemented in many European and North American cities,<sup>12–17</sup> most of which focus on gas leak location and gas facility emissions, but there is a gap in the literature for South East Asian mobile methane studies, and studies which combine multiple methods of source characterization.

Isotopic measurements of methane are used for source attribution and can provide insight into whether unknown sampled sources of methane are biogenic, thermogenic or pyrogenic in origin.<sup>18</sup> C<sub>2</sub>H<sub>6</sub>:CH<sub>4</sub> ratios can also be used to distinguish emission sources. Ethane is typically coemitted with methane in thermogenic and pyrogenic sources, but is generally absent in biogenic emissions.<sup>19</sup>

**Received:** February 20, 2025  
**Revised:** October 10, 2025  
**Accepted:** October 14, 2025  
**Published:** November 11, 2025



Since 2007, there has been renewed growth in global atmospheric CH<sub>4</sub> mole fractions following a 7-year plateau. This increase in methane mole fraction was coupled with a global shift to more negative  $\delta^{13}\text{C}$  values.<sup>20–22</sup> Methane mole fraction and  $\delta^{13}\text{C}$  measurements are commonly used to study the methane budget at global and regional scales, but the lesser measured  $\delta^2\text{H}$  can be used as a third dimension.<sup>18</sup>

Vietnam has signed the Global Methane Pledge and has published a Methane Action Plan 2030.<sup>23</sup> The realization of the methane mitigation ambitions set out in these plans will require the successful monitoring of methane emissions. This will require improved measurement, identification and quantification of methane sources. Initiatives such as these underscore the urgency and relevance of the study, aligning it with broader national and global mitigation efforts.

We demonstrate that a combination of stationary and mobile measurements allows for characterization of methane sources in large urban areas, which can in some cases then be verified by satellites. Here, we present measurements of methane and ethane mole fraction,  $\delta^{13}\text{C}\text{-CH}_4$ , and  $\delta^2\text{H}\text{-CH}_4$  from Ho Chi Minh City (HCMC), Vietnam's largest populated city of almost 9 million people.

## METHODS

A combination of three methodologies; stationary in situ observations between 2018 and 2019, urban vehicle surveying and spot sampling over 4 days in March 2023, and satellite observations in 2022 and 2023, were used to identify methane sources in HCMC, Vietnam.

### Continuous Stationary Measurements of Methane and Ethane in HCMC (2018–2019)

Continuous stationary measurements of methane and ethane and carbon dioxide mole fractions were made between 2018/10/01 and 2019/04/01 from the roof of an 11-story (60 m height) building operated by the Faculty of Environment, University of Science in HCMC, located at 10°45'45"N, 106°40'56"E (shown as the yellow square in Figure 2), in the framework of a large campaign focused on air quality reported in Hien et al.<sup>24</sup> The measurements were taken from the top of a 15 m mast located on the roof of the University building in a down-town area of HCMC surrounded by residential, transport and commercial activities. Measurements of methane and carbon dioxide were also carried out continuously (1 min) with a Los Gatos CO<sub>2</sub>/CH<sub>4</sub> Integrated Cavity Output Spectrometer (ICOS) (model no. 907-0010). Hourly measurements of ethane were performed using a Gas Chromatograph equipped with a Flame Ionization Detector (GC-FID); the limit of detection for ethane measurements on this instrument is 29.98 ppt. Methane measurements were collected as a supporting measurement and the high mole fractions observed formed the motivation to map methane sources in HCMC and subsequently continuous stationary methane mole fraction measurements were carried out in March 2023. For more information on the measurements taken as part of the 2018–2019 study see Hien et al.<sup>24</sup>

### 2023 Mobile Measurements

**Mobile Methane and Ethane Measurements.** We performed a mobile survey of methane and ethane mole fractions between 2023/03/20 and 2023/03/24 using a Los Gatos Research (LGR) Ultraportable CH<sub>4</sub>/C<sub>2</sub>H<sub>6</sub> ICOS Analyzer (uMEA, measurement rate 1 Hz). The precision of CH<sub>4</sub> measurements (1 $\sigma$ , 1 s averaging) is 0.9 ppb, and 20 ppb

for C<sub>2</sub>H<sub>6</sub>. The calibrated range for ethane is 0–1 ppm ethane and 0–10 ppm for methane. The flow response time is <0.4 s (1/e). This instrument uses off-axis integrated cavity output spectroscopy (OA-ICOS).

The sampling inlet was located on a vehicle roof and connected to the instrument using 3 m of 1/4" polyurethane tubing. The vehicle position was continuously recorded using a Navilock NL-602U USB GPS receiver. During the mobile survey, we collected approximately 20 h of high-frequency (1-Hz) methane data to obtain a broad overview of emission types across the contrasting zones of the city, this was supplemented with the measurement of ethane, which offers insights into specific source types.

Excess C<sub>2</sub>H<sub>6</sub>:CH<sub>4</sub> ratios were calculated from the LGR uMEA data. To calculate the excess mole fraction, background values were established by calculating the mean of the lowest 2 percentile of mole fraction data for each of the days. The slope of C<sub>2</sub>H<sub>6</sub> excess vs CH<sub>4</sub> excess was calculated for running 5 min intervals for each data point. Data with a correlation coefficient below 0.9 were discarded. This method is also used in studies such as Fernandez et al.,<sup>15</sup> Lowry et al.<sup>19</sup>

The mobile survey route was determined with the help of researchers who live in HCMC. Potential major sources (such as landfills and canals) were noted and the survey was designed to cover these, as well a variety of areas which are typical of large cities, such as major roads, commercial areas, industrial areas, residential areas, urban and congested areas. Across the survey approximately 440 km of road was covered.

**Isotopic Measurements.** To further aid methane source characterization during the mobile survey, we collected discrete samples for offline isotope analysis from a range of methane sources including: compressed natural gas (CNG) from a bus station and a CNG station, sewage, urban waterways, road transport (mainly mopeds), mangroves and a landfill. Discrete samples were collected in 5 L or 10 L Supel-Inert Multi-Layer Foil bags which were filled using a 6 V diaphragm pump (KNF: NMP830 KPDC). Samples were dried during the filling procedure using magnesium perchlorate. Samples are collected very close to the source (closer than 1 m) and then at further periodic distances from the source (up to around 5–10 m), so that a wider range of mole fractions can be measured, and therefore a better linear fit can be achieved for the Keeling plot analysis. Photographs of the collection of some of the samples can be seen in Figure S1.

The bags were measured at the Royal Holloway University of London (RHUL) Greenhouse Gas Laboratory for CH<sub>4</sub> mole fraction on a G2301 cavity ring-down analyzer (Picarro Inc.), to the World Meteorological Organization X2004A scale, and for  $\delta^{13}\text{C}$  on a Isoprime Trace Gas using isotope ratio mass spectrometry (IRMS),<sup>25</sup> where 75 mL of air is required for each measurement. The Isoprime Trace Gas IRMS measures  $\delta^{13}\text{C}\text{-CH}_4$  to high precision ( $\pm 0.05\%$ ). A selection of these sample bags were measured for  $\delta^2\text{H}$  of CH<sub>4</sub> using IRMS at the Institute for Marine and Atmospheric research Utrecht (IMAU), Utrecht University.<sup>26</sup> Methane was extracted from 60 mL of air which was extracted from the 5/10 L sample bags for each  $\delta^2\text{H}$  measurement (Instrument IVAN-XP) which also measures to a high precision of  $\pm 1.5\%$ . Samples with methane mole fraction over 7 ppm at RHUL, and 3 ppm at IMAU were diluted with pure nitrogen to ensure the sample peaks on the mass spectrometer were in the linear range. For  $\delta^{13}\text{C}$ , values are relative to the international standard materials Vienna

Peedee Belemnite (VPDB) and for  $\delta^2\text{H}$  to the Vienna Standard Mean Ocean Water (VSMOW).

The  $\delta^{13}\text{C}$  and  $\delta^2\text{H}$  source signatures are calculated using the Keeling plot analysis.<sup>27,28</sup> For the linear fit, the bivariate correlated errors and intrinsic scatter method (BCES) is used to calculate the  $y$ -axis intercept, which represents the isotopic source signature of the source, and its errors.<sup>29,30</sup> The BCES method was designed for a linear extrapolation to the  $y$ -axis. This method uses the uncertainties of the measurements to calculate the uncertainty on the source signature by accounting for correlated errors between the two variables.<sup>30</sup>

**Calibration.** The  $\text{CH}_4/\text{C}_2\text{H}_6$  LGR uMEA is calibrated against two standards which have been measured to have methane mole fractions of 9.7 and 1.85966 ppm. One is a cylinder of dry air which has values of  $\text{CH}_4$  and  $\text{CO}_2$  assigned by the NOAA central calibration laboratory in Boulder, US. The other standard has values of  $\text{CH}_4$  and  $\text{C}_2\text{H}_6$  given by BOC UK. The BOC values are less precise but a higher mole fraction is needed for the calibration of high mole fraction measurements from source studies. For ethane measurements on the same LGR uMEA, the high BOC cylinder is also used for calibration, as well as a cylinder with ambient air, with mole fraction values of 1 ppm and 1 ppb, respectively. A two point calibration is carried out by plotting the given value of the calibration gas against the value measured by the LGR uMEA. The equation of the line of best fit of these points is then used to adjust the measurements outputted from the instruments during the field campaign. This calibration is carried out pre and post campaign.

For the Isoprime Trace Gas IRMS, reference cylinders are used for calibration and correction so that measurements are on the VPDB scale. Isotopic measurements are made relative to a reference  $\text{CO}_2$  BOC gas cylinder, analyzed in the mass spectrometer in every run. A cylinder of air from NOAA, a sample of which has been analyzed at Institute of Arctic and Alpine Research, is used to standardize a working standard at RHUL, named RHS. RHS is analyzed as a sample on the Isoprime trace gas, three times in the morning, and then once between every two samples measured throughout the day, and lasts for around one year. Another cylinder from NOAA is run every few months to check for long-term drift, as well as when the RHS tank is changed. Additionally, another tank from NOAA is measured once a week as a target gas to ensure that the measurements are stable. A blank is also run and corrected for. Umezawa et al.<sup>31</sup> carried out a global interlaboratory analysis which involved the round robin of a cylinder which was measured and compared at each institution, from this it was found that there is a 0.2‰ offset between RHUL and INSTAAR, so this correction is applied to all of the  $\delta^{13}\text{C}$  measurements.

For the  $\delta^2\text{H}$  measurements on IVAN-XP, one point calibrations are carried out with a reference cylinder which has a  $\delta^2\text{H}$  value of  $-90.91\text{‰}$  (VSMOW) and a  $\delta^{13}\text{C}$  value of  $-48.09\text{‰}$  (VPDB) assigned to it. For more details on calibration see Brass and Röckmann.<sup>26</sup>

For the 2018/2019 stationary measurements, methane and carbon dioxide mole fractions were determined using Integrated Cavity Output Spectroscopy (ICOS, Los Gatos Research, LGR: 907-0010). The analyzer was calibrated every 23 h with gas reference standards prepared at the Max Plank Institute for Biogeochemistry GasLab and are traceable to World Meteorological Organisation internationally recognized calibration scales, namely, WMO X2004A and WMO  $\text{CO}_2$

X2007 for  $\text{CH}_4$  and  $\text{CO}_2$ , respectively. The analyzer output was corrected for instrumental drift between calibrations using a working reference cylinder, consisting of dry ambient air, which was introduced to the analyzer every 6 h. Calibration and drift corrections were applied instantaneously to the analyzer output using bespoke software designed at the University of East Anglia. High frequency measurements (1 Hz) were averaged over 5 min to achieve a precision better than  $\pm 0.5$  ppm for  $\text{CO}_2$  and  $\pm 5$  ppb for  $\text{CH}_4$ . We note that these precisions would not be suitable for measurements in rural or remote regions where WMO precision goals would be desirable. However, the reduced precision was sufficient as the deviations from 'background' mole fractions were several orders of magnitude above this WMO precision goal. The isotopic and mole fraction data from 2023 as well as the time series from 2018 to 2019 can be accessed at doi: 10.17632/f7cgwnySyn.1.

### Satellite Measurements

PRecursore IperSpettrale della Missione Operativa (PRISMA) is a hyperspectral imaging satellite operated by the Italian Space Agency that measures in the spectral range of 400–2505 nm with a spectral resolution of  $\leq 12$  nm. Based on the basic principle of imaging spectroscopy, measurements of reflected solar radiation from the Earth's surface in the short-wave infrared region (around 1650 and 2300 nm) can be used to retrieve methane concentration enhancements. However, this technique is spatially and temporally limited to the satellite's overpass times and is strongly constrained by atmospheric conditions, particularly cloud cover and humidity—challenges that are frequent in tropical regions.

Clear-sky Level 1B (calibrated Top of Atmosphere radiance) images of methane plumes in HCMC were retrieved from the PRISMA satellite archive, available since 2019. The archives of NASA's Earth Surface Mineral Dust Source Investigation (EMIT) mission, located on the International Space Station, and the German Aerospace Center (DLR) mission, The Environmental Mapping and Analysis Program (data available from July and October 2022, respectively) were also checked, but at the time of the study, there were still no images available over the study area.

Methane enhancement retrievals in these images were performed using the Matched Filter (MF) technique,<sup>32–34</sup> adapted to PRISMA's spectral configuration,<sup>35</sup> and further refined by Roger et al.<sup>36</sup> to reduce the occurrence of retrieval artifacts and background noise. The MF methods aim to detect the methane absorption signature (the target spectrum) across a hyperspectral image using data-derived statistics. Using a look-up table of radiative transfer simulations generated with the MODTRAN radiative transfer code,<sup>37</sup> a unit methane absorption spectrum has been calculated, representing the change in radiance for a 1 ppm increase in methane concentration per 1 m path length. With the unit absorption spectrum, the MF translates the changes in the radiance to methane enhancement in ppm-m units. An 8 km height is assumed to get the  $\text{CH}_4$  concentration enhancement ( $\Delta\text{XCH}_4$ ) in ppm units.<sup>38</sup> To account for across-track variations in the instrument's radiometric and spectral response, the statistics needed by the MF (the mean spectrum and covariance matrix) are computed per image column. The retrieval is applied for all the pixels in the image, producing the  $30 \times 30 \text{ km}^2$   $\Delta\text{XCH}_4$  maps that PRISMA images cover with 30-m resolution.

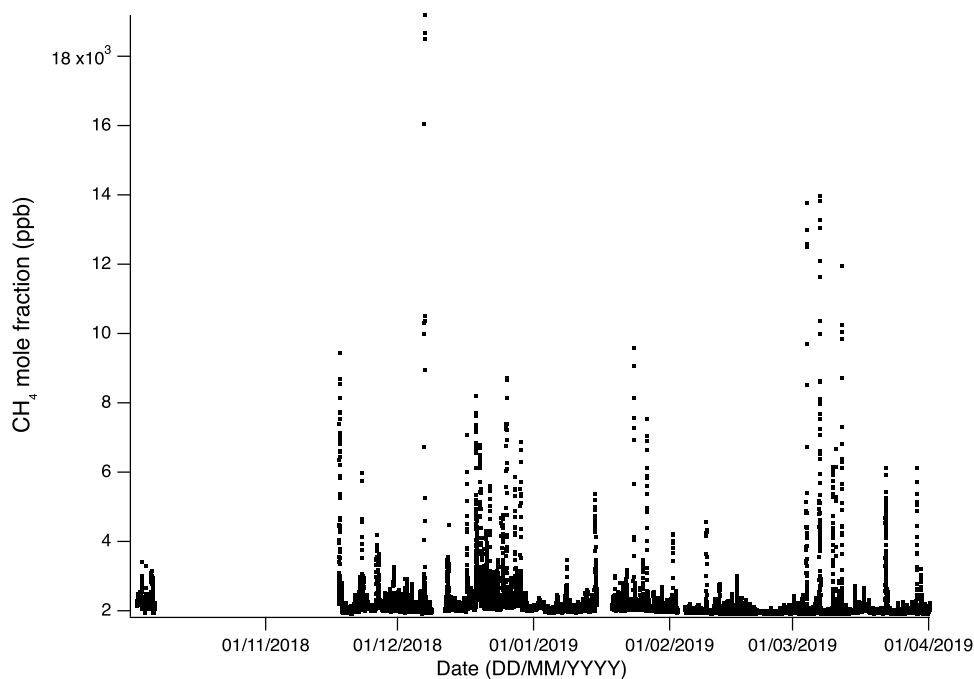


**Figure 1.** Time series of methane mole fraction collected in 2018–2019 on the roof the 11th floor of the Faculty of Environment, University of Science building in HCMC, located at  $10^{\circ}45'45''\text{N}$ ,  $106^{\circ}40'56''\text{E}$ .

The detection of methane plumes in the resulting  $\Delta\text{XCH}_4$  maps is performed by visual inspection to distinguish enhancements correlated with surface features (false positives) from true positives.<sup>35,39,40</sup> The latter are characterized by clusters of pixels with high concentrations of methane (above the median value of the image considered as the background value) that form the characteristic plume shape of emissions detectable from high-resolution satellites, which are not correlated with any other surface artifact, and the direction of the plume coincides with the direction of the wind. If there are multiple images of the area of interest, the identification of plumes is facilitated as they change shape and direction depending on the wind, reaffirming their lack of connection with surface features. Although other independent pixels with enhancement present in PRISMA images may indeed be minor emissions from other sources, given the high number of false positives in typical PRISMA images, there is no way to validate them as emissions without additional ground information. Once the plumes in each image have been identified, they are manually masked to ensure that no false positives are included in the mask.

The methane emission flux ( $Q$ ) was estimated using the Integrated Methane Enhancement (IME) method adapted to PRISMA as described by Guanter et al. This approach integrates the amount of methane within the masked plume (IME) in kg, the plume length scale ( $L$ ) in  $\text{m}^2$ , and the effective wind speed ( $U_{\text{eff}}$ ) in  $\text{m/s}$  to obtain a flux rate estimation. The  $U_{\text{eff}}$  is calculated as a linear function of the 10 m wind speed ( $U_{10}$ ), derived from large-eddy simulations that reflect the characteristics of methane plumes under typical satellite overpass conditions. The 1 h average 10 m wind ( $U_{10}$ ) data is taken from the NASA Goddard Earth Observing System – Forward Processing (GEOS-FP) meteorological reanalysis product at  $0.25^{\circ} \times 0.3125^{\circ}$  resolution. The uncertainty in  $Q$  was estimated by propagating the errors in wind speed ( $U_{10}$ ) and integrated methane enhancement (IME), following an

approach similar to that of Cusworth et al.<sup>41</sup> A conservative 50% uncertainty was assumed for the GEOS-FP  $U_{10}$  values, consistent with previous studies.<sup>39,42</sup> For each plume, a random distribution of wind speeds was generated around the actual  $U_{10}$  value, and the corresponding  $Q$  values were calculated using the measured IME and plume length ( $L$ ). The standard deviation of the resulting  $Q$  distribution was taken as the  $1 - \sigma$  uncertainty of the flux estimate. The wind speed and IME contributions were then combined quadratically to obtain the total uncertainty.

The two PRISMA images considered in this work are the only observations available from open-access high-resolution satellite missions with enough sensitivity to detect landfill emissions at the time of the study<sup>43</sup> that allowed a clear characterization of the methane emission. In addition to these two images, a third cloud-free image from January 14, 2022 was found in the PRISMA archive, where it is possible to observe a methane enhancement over the landfill, but given the wind direction (west), the plume tail is mixed with surface artifacts (mainly buildings surrounding the landfill to the west), which disturb the signal obtained from the satellite and hinder a clear characterization of the plume. Given these conditions, we consider that it is not possible to accurately quantify the emission in the January 14, 2022 observation, and we discard the image for this study.

## RESULTS

### 2019 Methane and Ethane Data

Continuous methane mole fraction measurements revealed extremely elevated methane mole fractions in the early hours (04:00–07:00 AM) that lasted between 1 and 3 h. The maximum elevation observed in the 5 min averaged data was approximately 18 ppm above the background mole fractions, see Figure 1. These plumes formed part of the motivation to carry out mobile measurements of  $\text{CH}_4$  and collect samples for

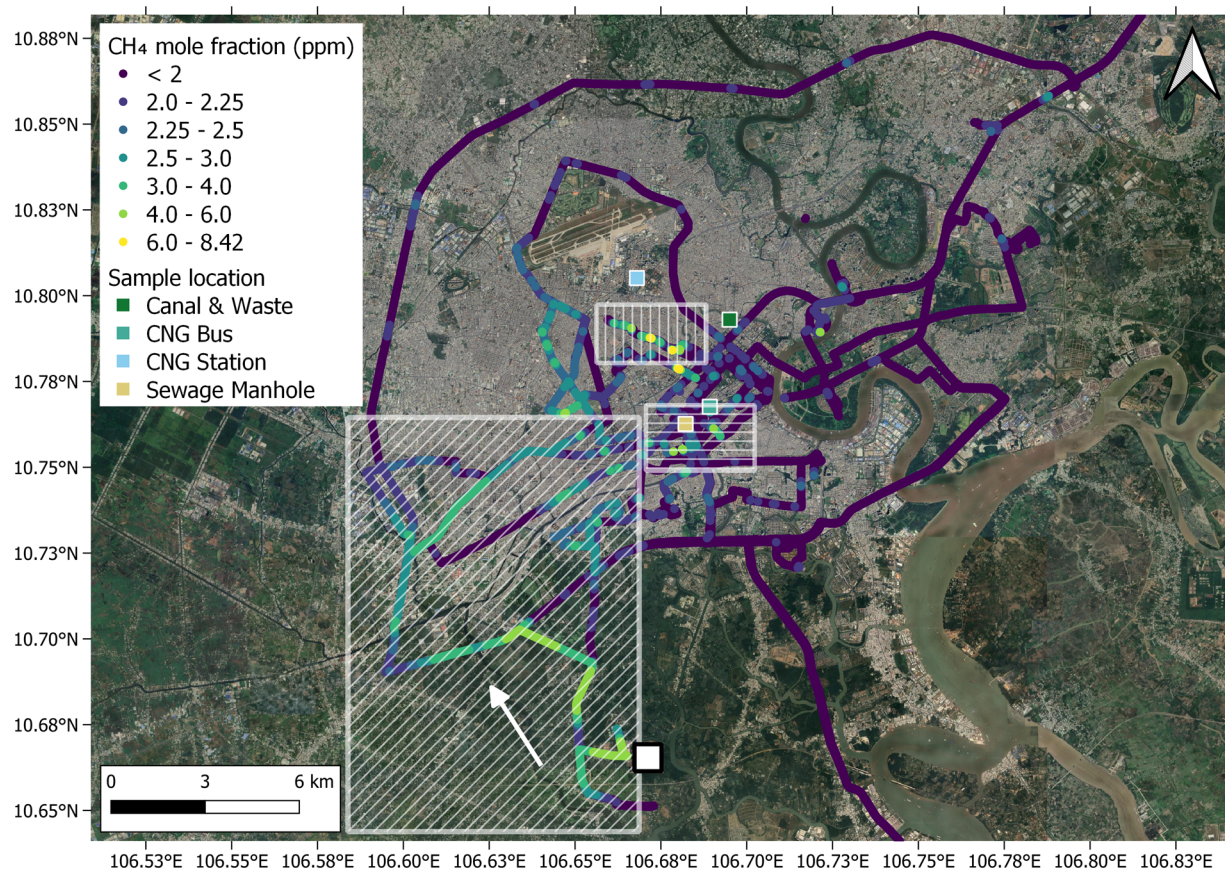


**Figure 2.** CH<sub>4</sub> mole fraction track in HCMC, Vietnam measured with an LGR uMEA. The results of 4 days of mobile vehicle surveying from 2023/03/20 to 2023/03/23 are combined. Winds were consistently SSE across the 4 days of surveying, represented by the white arrow (also see Figure S5 for wind rose plot). The diagonally hashed rectangle highlights atmospheric CH<sub>4</sub> mole fractions which are elevated above background due to emissions from the Da Phuoc landfill, located by the white square. The vertically hashed rectangle outlines increased CH<sub>4</sub> mole fraction in the vicinity of the Nhieu Loc–Thi Nghe Channel waterway. The horizontally hashed box highlights a number of localized CH<sub>4</sub> sources in the most heavily congested area with major traffic intersections. Locations of bag sample collection for isotopic analysis are also shown with smaller squares. The yellow square also represents the location at which the long-term measurements were taken. Background image from Google satellite.

isotopic analysis, in order to identify the source of these large and consistent plumes.

Enhancements in ethane were observed daily around 6 am and 6 pm, corresponding to rush hour traffic times. See Figure S2 for the ethane mole fraction time series in March 2019. A wind rose plot for this period of measurements can be seen in Figure S3. The peaks in methane were not always collocated temporally with the ethane emission events (see Figure S4), which indicates that the large methane enhancements could be from a biological source.

The findings from the mobile survey carried out in March 2023, highlighted in the following section, further support the hypothesis that the increased methane observed in the 2018–2019 in situ observations is consistent with the accumulation of emissions into a shallow boundary layer from a large biogenic source, such as a landfill, and its subsequent advection into HCMC.

### 2023 Mobile Measurements of CH<sub>4</sub> in HCMC

This section presents the findings of CH<sub>4</sub> and C<sub>2</sub>H<sub>6</sub> mole fraction and  $\delta^{13}\text{C}-\text{CH}_4$  and  $\delta^2\text{H}-\text{CH}_4$  measurements collected in HCMC in March 2023. For  $\delta^{13}\text{C}$  each source signature is distinct from the other (with the exception of the CNG and canal signatures), with no overlap within the errors on these signatures (calculated from BCES fit to Keeling plot data). However,  $\delta^2\text{H}$  was less effective in separating the sources

than  $\delta^{13}\text{C}$ : landfill and sewage signatures are not obviously distinct, and both the moped and canal signatures have a higher spread around atmospheric background. See Figure 3 for Keeling plots for both isotopic ratios.

**Landfill Emissions.** Figure 2 shows the track of the mobile measurements in HCMC in March 2023, color coded with the observed CH<sub>4</sub> concentration. Three regions of significantly elevated CH<sub>4</sub> plumes were observed. The diagonally hashed rectangle in Figure 2 outlines the southwest area of the city where atmospheric CH<sub>4</sub> mole fractions were elevated above background due to emissions from the Da Phuoc landfill to the south of the city, indicated by the white square in Figure 2. The wind directions throughout the surveying period were primarily SSE (see wind rose plot in Figure S5). The data show enhancements of over 1 ppm for large transects of the city approximately 15 km downwind of the landfill. Ethane, which can be used as a tracer to distinguish between biogenic and thermogenic sources, was not observed in these plumes, indicating a biogenic source.

The  $\delta^{13}\text{C}$  source signature calculated from targeted discrete sampling in close vicinity to the Da Phuoc landfill was  $-55.5 \pm 0.1\text{‰}$  (see Figure 3 for all Keeling plot results). This source signature is in close agreement with the source signature calculated from samples collected across the city during the mobile survey while in the large plume,  $-55.1 \pm 0.1\text{‰}$ , which

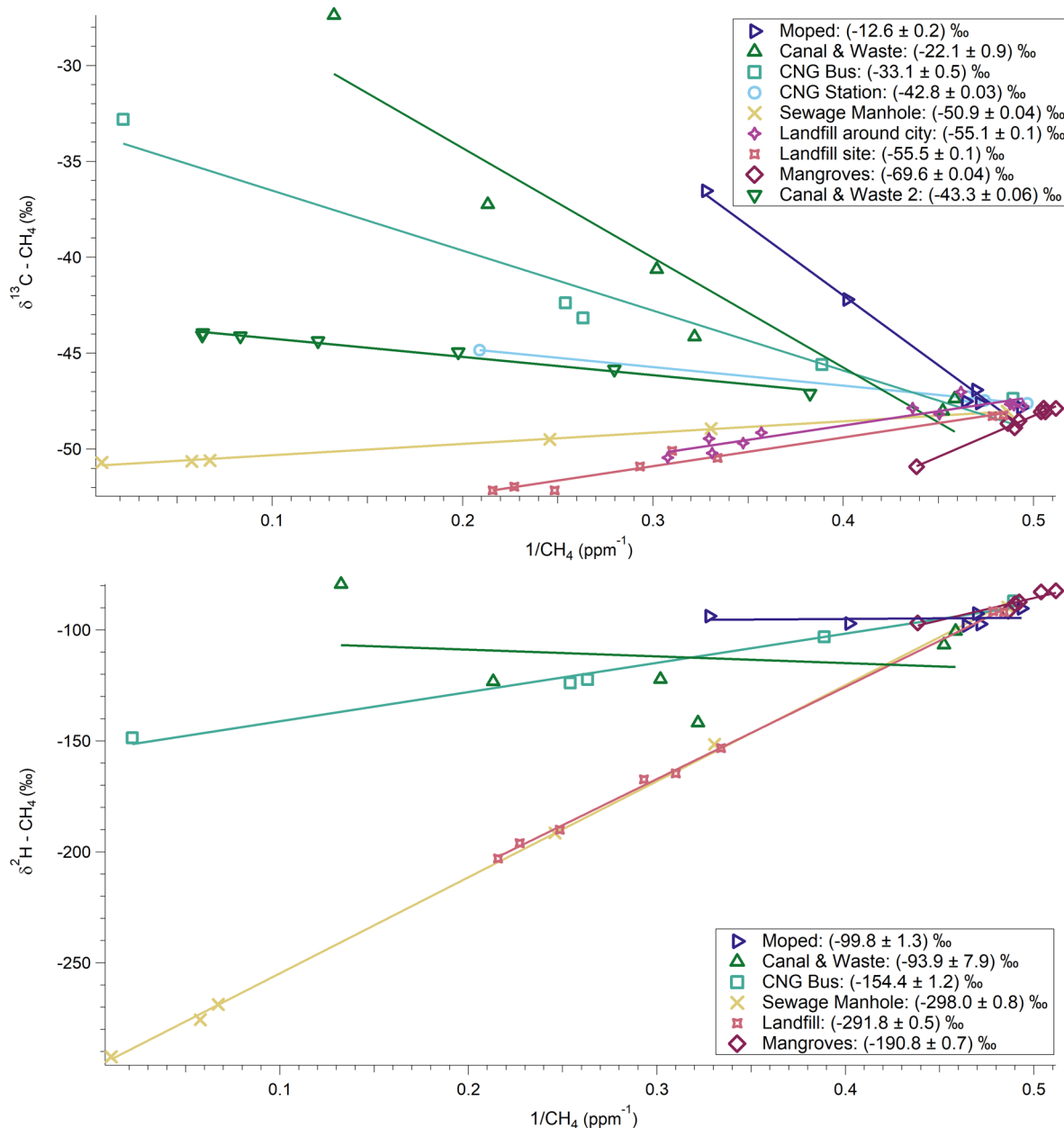


**Figure 3.** Keeling plots of spot samples collected at seven sources around HCMC and analyzed at RHUL, UK. The  $\delta^{13}\text{C}-\text{CH}_4$  source signatures, calculated from the  $y$ -intercept of the BCES fit are shown in the legend of the top panel. The  $\delta^2\text{H}-\text{CH}_4$  source signatures are shown in the legend of the bottom panel, for which samples were analyzed at IMAU, Utrecht University. Error bars are not visible at this scale.

confirms that the source of the extended and broad plumes observed across the city can be attributed to this landfill in the south of the city. This landfill was approximately 10 km from the stationary site where measurements were taken in 2018–2019. The significant biogenic enhancements observed in these mobile measurements suggest that the enhancements of methane seen during 2018–2019 were likely due to the Da Phuoc landfill.

**Emissions from Traffic.** The horizontally hashed box in Figure 2 highlights a number of smaller and more localized  $\text{CH}_4$  sources which are associated with colocated ethane emissions. These were most prevalent at major intersections with heavy traffic. Figure 4 highlights the high ethane to methane ratio that was observed in HCMC. Samples for isotopic analysis taken behind the exhaust of a stationary moped revealed a  $\delta^{13}\text{C}$  source signature of  $-12.6 \pm 0.2\text{‰}$  that

is typical of inefficient combustion.<sup>18</sup> The  $\delta^2\text{H}$  signature for the moped ( $-99.8 \pm 1.3\text{‰}$ ) was close to atmospheric background, despite the elevation recorded of over 1 ppm from background, measured when the moped was in a low gear, at low revs

An average  $\text{C}_2\text{H}_6:\text{CH}_4$  ratio of  $0.57 \pm 0.14$  was recorded on roads around HCMC. Such elevated ratios have only previously been noted from incomplete combustion events.<sup>19</sup> The spread in the  $\text{C}_2\text{H}_6:\text{CH}_4$  values calculated for each emission event, could be attributed to differences in engines, e.g., older engines may have more incomplete combustion since newer engines are more efficient. Emissions of methane that were coemitted with ethane were attributed to traffic emissions across the city, likely due to the dominance of mopeds in the traffic fleet. Figure S6 in the Supporting Information shows other examples of colocated emissions of

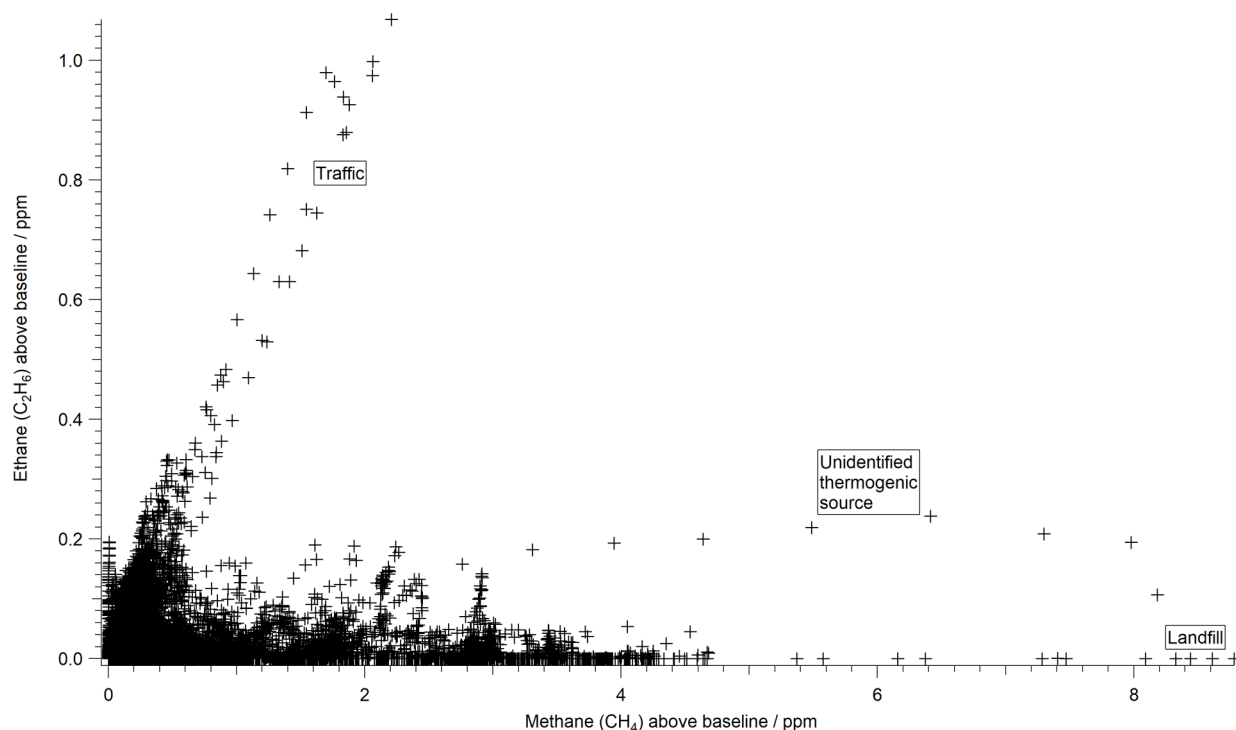


**Figure 4.** Methane plotted against ethane from data collected during day three of an urban mobile campaign in Ho Chi Minh City. A linear relationship between the two was observed here for traffic emissions, while driving through a tunnel, and throughout the city. Methane elevations with no ethane emissions coemitted can be seen along the *y*-axis of this figure, which correspond to landfill emissions. The area between the traffic and landfill lines is an example of the large number of periods where traffic influence is overlain on the landfill emissions, making it difficult to untangle without the ethane tracer.

$\text{CH}_4$  and  $\text{C}_2\text{H}_6$  that were observed while driving in highly congested areas which also demonstrates their high  $\text{C}_2\text{H}_6:\text{CH}_4$  ratios.

Other traffic related sources were also investigated; the collection of samples at a CNG bus and CNG refilling station resulted in the source signatures for  $\delta^{13}\text{C}$  and  $\delta^2\text{H}$  presented in Figure 3. Both signatures are enriched in the heavier isotope. The methane isotopic signature of natural gas in Vietnam, or specifically the HCMC region, has never been measured before, and thus this study provides the isotopic characteristics of natural gas in this area, which are consistent with thermogenic source characteristics. For  $\delta^{13}\text{C}$ , the CNG bus signature is more enriched than the signature from the CNG refilling station, which is consistent with combustion of the source.<sup>44</sup>

It should be noted that despite mopeds and buses both being forms of transport, the mechanisms under which they emit methane (with certain isotopic signatures) is not the same. Combustion preferentially consumes isotopically lighter natural gas, so the remaining methane leaking from CNG bus exhaust is isotopically heavier. The methane leakage from CNG buses only involves isotopic fractionation from the partial combustion of methane. In comparison, the mechanism for methane emissions from mopeds instead involves isotopic fractionation from the incomplete combustion of gasoline producing methane. This distinction explains why their carbon isotopic values differ.

**Canal Emissions.** The vertically hashed rectangle in Figure 2 corresponds to increased  $\text{CH}_4$  mole fraction in the vicinity of the Nhieu Loc–Thi Nghe Channel waterway. The lack of ethane present in these plumes indicates that this source is biogenic in nature, likely from the above-ground wastewater

system pipes which run along the canal, or emissions from the canal itself. The region of the canal which was sampled had waste floating on the surface, and the corresponding  $\delta^{13}\text{C}-\text{CH}_4$  source signature of  $-22.1 \pm 0.9\%$  is unusual. Biogenic sources such as canals and landfills are usually depleted in  $^{13}\text{C}$ ; a signature of  $-22\%$  is more comparable to methane emissions from fire or vehicle combustion.<sup>45</sup> It is difficult to disentangle this complex source mix, but possible explanations include emissions from plastic<sup>46</sup> or, the  $\delta^{13}\text{C}$  signature observed here is similar to those recorded in Klintzsch et al.<sup>47</sup> for methane released from phytoplankton. Five out of six phytoplankton species investigated in this study produced  $\text{CH}_4$  that was enriched in  $^{13}\text{C}$  relative to atmospheric  $\text{CH}_4$   $\delta^{13}\text{C}$  values. The source signature, calculated from Keeling plot analysis, ranged between  $-1$  and  $-43\%$ . Although the sample bags were filled between 20 cm to 5 m from the water, it should be noted that there is the possibility that methane from other sources could potentially have been transported and concentrated over the waterways, therefore “contaminating” the canal sample. That being said, regardless of the source, there is a high buildup of methane along the canals, which should be considered in mitigation strategies.

Resampling of the same location took place on 2023/09/29, during the end of the rain season, when the waste floating on the canal was visibly degraded compared to sampling at the end of the dry season. The  $\delta^{13}\text{C}-\text{CH}_4$  source signature for the second analysis was  $-43.3 \pm 0.06\%$ . The signature is more depleted than seen in the dry season months, and is typical of methane from sewage treatment following partial oxidation.<sup>48</sup> The change in the source signature could be a result of the changes in environmental conditions mentioned.

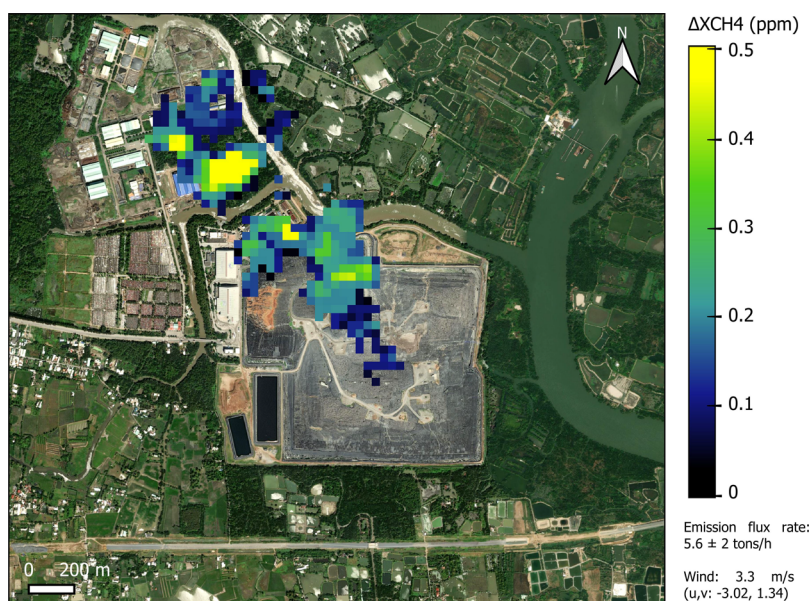


**Figure 5.** Methane emission plume from the Da Phuoc landfill observed by the PRISMA satellite on 2023/02/13, at a rate of  $5.6 \pm 2$  tonnes/h, background image from Bing Aerial.

The  $\delta^2\text{H}$  signature for this source has a large uncertainty, with a spread of measurements that do not show as clear of a correlation as other sources, which could be due to the complex source mix within the canal at this location.

**Mangroves.** Air samples were also taken in the Can Gio mangroves around  $10^\circ 30' 4,212''\text{N}$   $106^\circ 52' 14,034''\text{E}$ ,  $\sim 36$  km SE of the university building. The mangroves are a UNESCO Biosphere Reserve in the Can Gio District of HCMC. Samples for isotopic analysis were taken at both high and low tide (8 samples taken at each). No significant increases in methane mole fraction were observed when sampling at high tide.

Studies including isotopic measurements of mangroves in tropical areas are not abundant in the literature, especially for  $\delta^2\text{H}$ . The  $\delta^2\text{H}$  source signature of  $-190.8 \pm 1.8\text{‰}$  measured at low tide in this mangrove region is more enriched compared to tropical freshwater wetlands<sup>49</sup> and is instead comparable to the signature obtained from the landfill here, see Figure 3.

The source signature for  $\delta^{13}\text{C}$  found here is in agreement with the value outlined in Brownlow et al.<sup>50</sup> for mangroves in Costa Rica, but more negative than measurements from Hong Kong. The enriched  $\delta^2\text{H}$  source signature for the mangroves at low tide is interesting, similar measurements could not be found in literature. The higher  $\delta^2\text{H}$  signature of seawater present in the water in mangroves could lead to higher  $\delta^2\text{H}$  values in the methane emissions compared with tropical freshwater wetlands. Also due to the strong fractionation of hydrogen during oxidation, the enhanced oxidation of the produced methane in mangroves before emission to atmosphere would also increase  $\delta^2\text{H}$ .<sup>51</sup>

#### Satellite Data

The landfill is the largest source of atmospheric methane to HCMC observed in this study and impacts large parts of the city. To corroborate and validate the large enhancements of methane observed from the landfill in HCMC, publicly available methane-sensitive satellite data were analyzed. Methane emissions from the Da Phuoc landfill were also observed from space using the PRISMA satellite.<sup>35</sup>

Given the surface properties of the study area, i.e., heterogeneous surface, high water content lowering the surface radiance, vegetation, and surface artifacts such as buildings and roads that challenge the detection of methane emissions,<sup>35,36</sup> only hyperspectral satellites counting with higher sensitivity to methane are able to detect methane point source emissions among the available high-resolution satellites. At the time of the study, only the Italian PRISMA satellite had cloud-free images of Ho Chi Minh City in its archive. The available good-quality observations from 2022/10/21 and 2023/02/13 show a large methane plume from the southern landfill site in HCMC. Due to regular cloud cover, no other images are available.

For 2023/02/13, a methane emission of  $5.6 \pm 2$  tonnes/hour was derived from the remote observation, see Figure 5. During this satellite retrieval, the air was coming from the SSE, consistent with the airflow during the mobile measurement campaign. A plume was also detected on 2022/10/31 for which an emission rate of  $4.1 \pm 1.5$  t/h was estimated. The landfill was the only  $\text{CH}_4$  source that could be resolved by the PRISMA satellite in the HCMC region. The emission rate is comparable to emissions from other landfills that have been observed through satellite measurements, such as in Madrid with the GHGSat, the largest source here was releasing methane at a rate of  $\sim 5$  t/h.<sup>52</sup> And it is also of the same order of magnitude as the emissions reported in Maasackers et al.<sup>53</sup> for Buenos Aires, Delhi, Lahore, and Mumbai.

The remote observation of emissions from the landfill one and five months prior to the mobile campaign reveals that this emission event was not a one-off event that occurred only during the mobile campaign, and that this source is significant both temporarily, and in magnitude. This highlights that the landfill is a clear target for methane mitigation in HCMC, as well as for the mitigation of any other harmful gases committed from the landfill, which the city is repeatedly subjected to.

## DISCUSSION

### Summary

We have identified enhancements of methane and their sources in HCMC using three different methods: mobile measurements, continuous stationary measurements and satellite data. Together these highlight the sources of methane in this understudied region, and can inform future mitigation efforts.

During the 2023 campaign, mobile measurements of CH<sub>4</sub> and C<sub>2</sub>H<sub>6</sub> were made with an LGR uMEA. An absence of ethane elevations associated with large CH<sub>4</sub> elevations across the city was observed, which indicates a biogenic origin for this emission. These emissions were traced back to the Da Phuoc landfill site and elevations in methane from this source of over 1 ppm were observed over 15 km away. A characteristic C<sub>2</sub>H<sub>6</sub>:CH<sub>4</sub> value of 0.57 ± 0.14 was estimated for traffic emissions.

Additionally, samples were collected for isotopic analysis at a CNG bus and CNG station, sewage manholes, canal, moped, mangroves and landfill. These represent under studied sources in this region, and the isotopic measurements fill in gaps in global isotopic databases such as Sherwood et al.,<sup>18</sup> especially for δ<sup>2</sup>H. The dominant urban CH<sub>4</sub> sources in HCMC can effectively be differentiated with δ<sup>13</sup>C measurements, with δ<sup>13</sup>C ranging from −69.6‰ for mangroves to −12.6‰ for a moped. Hence, isotopic measurements allow for future source identification and tracking of CH<sub>4</sub> emissions in urban environments in Southeast Asia. However, δ<sup>2</sup>H is less useful for source characterization in HCMC than δ<sup>13</sup>C. This is in contrast to measurements that were made in Bucharest<sup>15</sup> and highlights the variability of CH<sub>4</sub> emissions between cities and the need for more measurements, since what is true for one area cannot necessarily be extrapolated to another. δ<sup>2</sup>H measurements are more sparse in the literature, and some of those reported here represent the first measurements for these source types.<sup>18</sup>

### Traffic Emissions

The significant traffic-related emissions of methane, coupled with enhancements in ethane, have not commonly been seen in previous urban methane mobile survey work in Europe, North America or Australia. In these locations the main sources of CH<sub>4</sub> are usually attributed to gas infrastructure, which is not present in HCMC, and waste.<sup>13,15,17</sup> Generally mopeds are not considered as a source of methane in global inventories, but regional differences in traffic profiles, such as those in South East Asia, need to be accounted for when considering regional methane emissions. For this identified source, there is the feasibility and possibility, relative to other sources, of reducing emissions via improved exhaust regulations.

### Landfill Emissions

The large emissions from landfills that were observed during the March 2023 campaign, were also observed in satellite data retrievals one and five months before this mobile campaign. This demonstrates that the emissions from the landfill were not just a one-off event that happened to be observed during the mobile campaign, but is a significant source of methane in HCMC temporally. Additionally, the wind direction during the 2018–2019 stationary measurements (see Figure S1) is also consistent with emissions from the same landfill, along with the fact that no ethane was observed with the high peaks of CH<sub>4</sub>,

the landfill may be the unknown source of methane responsible for the measurements that motivated this study.

The sustained emissions of methane from the landfill also raises concern of potential coemitted species, such as H<sub>2</sub>S and gases from leachate, and the effect this widespread and sustained exposure may have on the air quality and the millions of people in HCMC. A cobenefit of reducing methane emissions is the potential to also reduce coemitted gas species such as carbon dioxide and nonmethane volatile organic compounds, emitted from these sources.<sup>54</sup> HCMC is subjected to high concentrations of pollutants, some of which will come from the same sources as methane.<sup>55</sup> The byproducts of waste disposal have been found to be detrimental to human health in the surrounding areas as well as to the surrounding environment.<sup>56</sup> In their review of the health effects associated with the disposal of solid waste in landfills and incinerators in populations living in surrounding areas, Mattiello et al.<sup>57</sup> found that the most consistent effect is an increased risk of congenital anomalies and hospitalization due to respiratory disease nearby special waste landfills. Methane emissions can also have a detrimental effect on human health via ground level ozone production. Increases in surface ozone and fine particulate matter (PM<sub>2.5</sub>) are associated with excess premature human mortalities.<sup>58</sup> Given the long lifetime of CH<sub>4</sub>, this effect may be small at the local scale.

The observation of the landfill plume through both mobile and satellite measurements highlights that the source is significant enough to be observed in space, as well as the temporal persistence of this source. The temperature in HCMC is high enough for it to be emitting all year, but soil moisture content and atmospheric pressure will likely influence the magnitude of observed emissions, and this could be the focus of future work.

### Mitigation Opportunities

From the findings of this study, there are two clear mitigation opportunities that could be implemented in HCMC to reduce methane emissions. Emissions from landfills can be regulated using a variety of techniques. For example, a reduction in methane emissions from landfills can be achieved by means such as the implementation of biologically active covers,<sup>59</sup> inert and biogenic (food) separation<sup>60</sup> and methane capture and utilization on site<sup>61</sup> which can help to reduce the negative environmental and social impacts of landfills.<sup>62</sup> Additionally, more stringent exhaust regulations for mopeds could be implemented to reduce emissions that arise from incomplete combustion in motors. The use of two-stroke mopeds has also been noted to contribute to greenhouse gas emissions in Europe.<sup>63</sup> Four-stroke engine use significantly reduces methane emissions compared to two-stroke. Furthermore, the use of four-stroke mopeds can also result in improved urban air quality, resulting in lowered health risk and financial benefits to the health system.

### Future Suggestions for Methane Monitoring to Aid Mitigation Efforts

To understand which mitigation options are available, a detailed understanding of the different source types in a certain area is first required. Furthermore, a temporal understanding of these emissions is also useful, to observe the effects of mitigation strategies that are employed. For example, an understanding of seasonal trends will help to understand emissions, and long-term measurements are needed to quantify the success of mitigation strategies. Permanent/long-term

stationary measurements from a tall tower network, such as the Integrated Carbon Observation System in Europe or additional sites in the NOAA Global Monitoring Laboratory network around SE Asia, from background, urban, and suburban sites would be useful.

A protocol for reporting emissions, similar to oil and gas infrastructure, could be useful for landfill emissions. For example, this significant source could be better understood and monitored if operators could make their own measurements and use satellite data for corroboration. Hopkins et al.<sup>64</sup> highlight how urban methane mitigation will require new observations with a range of techniques, and new institutional partnerships.

The limitations of mobile methane measurements are that they are short-term, and not representative of long-term or seasonal changes in emissions. Similarly, satellite measurements depend on cloud coverage and overpass times, so the confirmation of these results with ground based measurements is important but is not frequently carried out.<sup>65</sup> This will become increasingly more viable with data from new satellites such as those in the Carbon Mapper program, or planned future missions such as CHIME (Copernicus Hyperspectral Imaging Mission for the Environment) or SBG (Surface Biology and Geology), which will result in improved observation and detection capabilities. The combination of these types of measurements could form a standard for future methane emission monitoring. Long-term stationary measurements are also important, as although they provide only limited insight into specific local sources, they can provide information on seasonal and long-term trends in emissions as well as into regional sources.<sup>66</sup> Developing links between each of these methods results in a clearer understanding of methane emissions in cities which do not have regular monitoring of this important greenhouse gas. Additionally, a local inventory for the city emissions would be valuable for the regulation and monitoring of greenhouse gases. The importance of understanding the spatial dependency of emissions is also becoming critical as measurement based inventories using satellite data are becoming more dependent upon spatially resolved inventories as priors.<sup>67</sup>

## CONCLUSIONS

The combination of urban mobile measurements and discrete sampling has resulted in the mapping and source attribution of the CH<sub>4</sub> sources in Ho Chi Minh City, Vietnam. Combined with stationary long-term and satellite measurements, there is evidence that efforts to mitigate methane in this city should target landfill emissions, since this source was seen to be the most significant across the three different measurement methods that spanned a 5 year study period.

Studies as reported here can help to formulate city-specific policies for methane emission reduction by providing focus on the sources actually contributing to the emissions rather than those presumed through emission factor inventory analysis. Our work demonstrates the feasibility and also the power of accurate source specific emission factors for inventories, which should be revisited regularly. Successful mitigation of methane sources and related policy making requires information on which sources to target, which can be achieved by mobile measurements, as well as long-term monitoring.

## ASSOCIATED CONTENT

### Supporting Information

The Supporting Information is available free of charge at <https://pubs.acs.org/doi/10.1021/acsestair.5c00034>.

The Supporting Information includes photographs taken during the collection of samples for isotopic analysis; ethane time series from 2019 taken at the stationary site at rush hours; wind rose for the period December 2018–April 2019 from the airport in HCMC during the period in which stationary measurements taken; methane and ethane time series from 2019; wind rose for the period 20–24 March 2023 from the airport in HCMC during the period in which mobile measurements taken around HCMC; and examples of isolated events where collocated emissions of CH<sub>4</sub> and C<sub>2</sub>H<sub>6</sub> observed (PDF)

HCMC (ZIP)

## AUTHOR INFORMATION

### Corresponding Authors

**Ceres A. Woolley Maisch** – Centre of Climate, Ocean and Atmosphere, Department of Earth Sciences, Royal Holloway, University of London, Egham TW20 0EX, U.K.;

orcid.org/0000-0002-5070-145X;

Email: [c.a.woolleymaisch@2uu.nl](mailto:c.a.woolleymaisch@2uu.nl)

**Rebecca E. Fisher** – Centre of Climate, Ocean and Atmosphere, Department of Earth Sciences, Royal Holloway, University of London, Egham TW20 0EX, U.K.;

Email: [r.e.fisher@rhul.ac.uk](mailto:r.e.fisher@rhul.ac.uk)

### Authors

**James L. France** – Centre of Climate, Ocean and Atmosphere, Department of Earth Sciences, Royal Holloway, University of London, Egham TW20 0EX, U.K.; Environmental Defense Fund, London EC3M 1DT, U.K.

**David Lowry** – Centre of Climate, Ocean and Atmosphere, Department of Earth Sciences, Royal Holloway, University of London, Egham TW20 0EX, U.K.

**Grant Forster** – Centre for Ocean and Atmospheric Science, School of Environmental Sciences and National Centre for Atmospheric Science, School of Environmental Sciences, University of East Anglia, Norwich NR4 7TJ, U.K.

**Thi Hien To** – Faculty of Environment, University of Science, Ho Chi Minh City 700000, Viet Nam; Vietnam National University Ho Chi Minh City, Ho Chi Minh City 700000, Viet Nam

**Itziar Irakulis-Loitxate** – Research Institute of Water and Environmental Engineering, Universitat Politècnica de València, Valencia 46022, Spain; orcid.org/0000-0003-3646-4950

**Nicholas Garrard** – Centre for Ocean and Atmospheric Science, School of Environmental Sciences, University of East Anglia, Norwich NR4 7TJ, U.K.

**Doan Thien Chi Nguyen** – Faculty of Environment, University of Science, Ho Chi Minh City 700000, Viet Nam; Vietnam National University Ho Chi Minh City, Ho Chi Minh City 700000, Viet Nam; orcid.org/0000-0002-6076-928X

**Thi Thanh Nhon Nguyen** – Faculty of Environment, University of Science, Ho Chi Minh City 700000, Viet Nam;

Vietnam National University Ho Chi Minh City, Ho Chi Minh City 700000, Viet Nam

**Hoang Minh Tran** – Faculty of Environment, University of Science, Ho Chi Minh City 700000, Viet Nam; Vietnam National University Ho Chi Minh City, Ho Chi Minh City 700000, Viet Nam

**Vo Tu Uyen Nguyen** – Faculty of Environment, University of Science, Ho Chi Minh City 700000, Viet Nam; Vietnam National University Ho Chi Minh City, Ho Chi Minh City 700000, Viet Nam

**Gia Luat Nguyen** – Faculty of Environment, University of Science, Ho Chi Minh City 700000, Viet Nam; Vietnam National University Ho Chi Minh City, Ho Chi Minh City 700000, Viet Nam

**Ha Phuc Duy Cao** – Faculty of Environment, University of Science, Ho Chi Minh City 700000, Viet Nam; Vietnam National University Ho Chi Minh City, Ho Chi Minh City 700000, Viet Nam

**Graham Mills** – Centre for Ocean and Atmospheric Science, School of Environmental Sciences, University of East Anglia, Norwich NR4 7TJ, U.K.

**David Oram** – Centre for Ocean and Atmospheric Science, School of Environmental Sciences, University of East Anglia, Norwich NR4 7TJ, U.K.

**Thomas Röckmann** – Institute for Marine and Atmospheric Research Utrecht, Utrecht University, Utrecht 3584 CC, the Netherlands; [orcid.org/0000-0002-6688-8968](https://orcid.org/0000-0002-6688-8968)

**Carina van der Veen** – Institute for Marine and Atmospheric Research Utrecht, Utrecht University, Utrecht 3584 CC, the Netherlands

**Euan G. Nisbet** – Centre of Climate, Ocean and Atmosphere, Department of Earth Sciences, Royal Holloway, University of London, Egham TW20 0EX, U.K.

Complete contact information is available at:  
<https://pubs.acs.org/10.1021/acsestair.5c00034>

## Notes

The authors declare no competing financial interest.

## ACKNOWLEDGMENTS

Measurements were funded through NERC project MethaneDH—NE/V000780/1 (Discovering reasons for global atmospheric methane growth using deuterium isotopes) and Leverhulme Grant EM-2024-054/4.

## REFERENCES

- (1) On Climate Change, I. P. Chapter 7: The Earth's energy budget, climate feedbacks, and climate sensitivity. In *Climate Change 2021: The Physical Science Basis. Contribution of Working Group I to the Sixth Assessment Report of the Intergovernmental Panel on Climate Change*, Masson-Delmotte, V., et al., Eds.; Cambridge University Press, 2021; pp 7–87.
- (2) Lan, X.; Thoning, K. W.; Dlugokencky, E. J. *Trends in globally-averaged CH<sub>4</sub>, N<sub>2</sub>O, and SF<sub>6</sub> determined from NOAA Global Monitoring Laboratory measurements*; NOAA Global Monitoring Laboratory, 2025.
- (3) Nisbet, E. G.; et al. Very Strong Atmospheric Methane Growth in the 4 Years 2014–2017: Implications for the Paris Agreement. *Global Biogeochemical Cycles* **2019**, *33*, 318–342.
- (4) Vo, T. B. T.; Wassmann, R.; Mai, V. T.; Vu, D. Q.; Bui, T. P. L.; Vu, T. H.; Dinh, Q. H.; Yen, B. T.; Asch, F.; Sander, B. O. Methane emission factors from vietnamese rice production: Pooling data of 36 field sites for meta-analysis. *Climate* **2020**, *8*, 74.

- (5) Pandey, A.; Mai, V. T.; Vu, D. Q.; Bui, T. P. L.; Mai, T. L. A.; Jensen, L. S.; de Neergaard, A. Organic matter and water management strategies to reduce methane and nitrous oxide emissions from rice paddies in Vietnam. *Agric., Ecosyst. Environ.* **2014**, *196*, 137–146.

- (6) Leon, A.; Minamikawa, K.; Izumi, T.; Chiem, N. H. Estimating impacts of alternate wetting and drying on greenhouse gas emissions from early wet rice production in a full-dike system in An Giang Province, Vietnam, through life cycle assessment. *Journal of Cleaner Production* **2021**, *285*, No. 125309.

- (7) Dušek, J.; Nguyen, V. X.; Le, T. X.; Pavelka, M. Methane and carbon dioxide emissions from different ecosystems at the end of dry period in South Vietnam. *Trop. Ecol.* **2021**, *62*, 1–16.

- (8) Vu, Q. D.; de Neergaard, A.; Tran, T. D.; Hoang, Q. Q.; Ly, P.; Tran, T. M.; Jensen, L. S. Manure, biogas digestate and crop residue management affects methane gas emissions from rice paddy fields on Vietnamese smallholder livestock farms. *Nutr. Cycl. Agroecosyst.* **2015**, *103*, 329–346.

- (9) Ishigaki, T.; Chung, C. V.; Sang, N. N.; Ike, M.; Otsuka, K.; Yamada, M.; Inoue, Y. Estimation and field measurement of methane emission from waste landfills in Hanoi, Vietnam. *J. Mater. Cycles Waste Manage.* **2008**, *10*, 165–172.

- (10) Bui, L. T.; Nguyen, P. H. Integrated model for methane emission and dispersion assessment from landfills: A case study of Ho Chi Minh City, Vietnam. *Sci. Total Environ.* **2020**, *738*, No. 139865.

- (11) Anh, L. H.; Thanh Truc, N. T.; Tuyen, N. T. K.; Bang, H. Q.; Son, N. P.; Schneider, P.; Lee, B. K.; Moustakas, K. Site-specific determination of methane generation potential and estimation of landfill gas emissions from municipal solid waste landfill: a case study in Nam Binh Duong, Vietnam. *Biomass Convers. Biorefin.* **2022**, *12*, 3491–3502.

- (12) Vogel, F.; et al. Ground-Based Mobile Measurements to Track Urban Methane Emissions from Natural Gas in 12 Cities across Eight Countries. *Environ. Sci. Technol.* **2024**, *58*, 2271–2281.

- (13) Ars, S.; Vogel, F.; Arrowsmith, C.; Heerah, S.; Knuckey, E.; Lavoie, J.; Lee, C.; Pak, N. M.; Phillips, J. L.; Wunch, D. Investigation of the spatial distribution of methane sources in the greater Toronto area using mobile gas monitoring systems. *Environ. Sci. Technol.* **2020**, *54*, 15671–15679.

- (14) Defratyka, S. M.; Paris, J. D.; Yver-Kwok, C.; Fernandez, J. M.; Korben, P.; Bousquet, P. Mapping Urban Methane Sources in Paris, France. *Environ. Sci. Technol.* **2021**, *55*, 8583–8591.

- (15) Fernandez, J. M.; Maazallahi, H.; France, J. L.; Menoud, M.; Corbu, M.; Ardelean, M.; Calcan, A.; Townsend-Small, A.; van der Veen, C.; Fisher, R. E.; Lowry, D.; Nisbet, E. G.; Röckmann, T. Street-level methane emissions of Bucharest, Romania and the dominance of urban wastewater. *Atmospheric Environment: X* **2022**, *13*, No. 100153.

- (16) Atherton, E.; Risk, D.; Fougère, C.; Lavoie, M.; Marshall, A.; Werring, J.; Williams, J. P.; Minions, C. Mobile measurement of methane emissions from natural gas developments in northeastern British Columbia. *Canada. Atmospheric Chemistry and Physics* **2017**, *17*, 12405–12420.

- (17) Maazallahi, H.; Fernandez, J. M.; Menoud, M.; Zavala-Araiza, D.; Weller, Z. D.; Schwietzke, S.; von Fischer, J. C.; Denier van der Gon, H.; Röckmann, T. Methane mapping, emission quantification, and attribution in two European cities: Utrecht (NL) and Hamburg (DE). *Atmos. Chem. Phys.* **2020**, *20*, 14717–14740.

- (18) Sherwood, O. A.; Schwietzke, S.; Arling, V. A.; Etiope, G. Global inventory of gas geochemistry data from fossil fuel, microbial and burning sources, version 2017. *Earth System Science Data* **2017**, *9*, 639–656.

- (19) Lowry, D.; Fisher, R. E.; France, J. L.; Coleman, M.; Lanoisellé, M.; Zazzeri, G.; Nisbet, E. G.; Shaw, J. T.; Allen, G.; Pitt, J.; Ward, R. S. Environmental baseline monitoring for shale gas development in the UK: Identification and geochemical characterisation of local source emissions of methane to atmosphere. *Science of The Total Environment* **2020**, *708*, No. 134600.

- (20) Nisbet, E. G.; et al. Rising atmospheric methane: 2007–2014 growth and isotopic shift. *Global Biogeochemical Cycles* **2016**, *30*, 1356–1370.
- (21) Zhang, Z.; Poulter, B.; Feldman, A. F.; Ying, Q.; Ciais, P.; Peng, S.; Li, X. Recent intensification of wetland methane feedback. *Nature Climate Change* **2023**, *13*, 430–433.
- (22) Rigby, M.; et al. Role of atmospheric oxidation in recent methane growth. *Proc. Natl. Acad. Sci. U.S.A.* **2017**, *114*, 5373–5377.
- (23) Viet Nam Action Plan for Methane Emissions Reduction by 2030. <https://www.iea.org/policies/17026-viet-nam-action-plan-for-methane-emissions-reduction-by-2030>.
- (24) Hien, T. T.; Huy, D. H.; Dominutti, P. A.; Thien Chi, N. D.; Hopkins, J. R.; Shaw, M.; Forster, G.; Mills, G.; Le, H. A.; Oram, D. Comprehensive volatile organic compound measurements and their implications for ground-level ozone formation in the two main urban areas of Vietnam. *Atmos. Environ.* **2022**, *269*, No. 118872.
- (25) Fisher, R.; Lowry, D.; Wilkin, O.; Sriskantharajah, S.; Nisbet, E. G. High-precision, automated stable isotope analysis of atmospheric methane and carbon dioxide using continuous-flow isotope-ratio mass spectrometry. *Rapid Commun. Mass Spectrom.* **2006**, *20*, 200–208.
- (26) Brass, M.; Röckmann, T. Continuous-flow isotope ratio mass spectrometry method for carbon and hydrogen isotope measurements on atmospheric methane. *Atmospheric Measurement Techniques* **2010**, *3*, 1707–1721.
- (27) Pataki, D. E.; Ehleringer, J. R.; Flanagan, L. B.; Yakir, D.; Bowling, D. R.; Still, C. J.; Buchmann, N.; Kaplan, J. O.; Berry, J. A. The application and interpretation of Keeling plots in terrestrial carbon cycle research. *Global Biogeochem. Cycles* **2003**, *17*, 1022.
- (28) Keeling, C. D. The concentration and isotopic abundances of atmospheric carbon dioxide in rural areas. *Geochimica et cosmochimica acta* **1958**, *13*, 322–334.
- (29) Akritas, M. G.; Bershad, M. A. Linear Regression for Astronomical Data with Measurement Errors and Intrinsic Scatter. *Astrophysical Journal* **1996**, *470*, 706.
- (30) Zazzeri, G.; Lowry, D.; Fisher, R. E.; France, J. L.; Lanoisellé, M.; Nisbet, E. G. Plume mapping and isotopic characterisation of anthropogenic methane sources. *Atmos. Environ.* **2015**, *110*, 151–162.
- (31) Umezawa, T.; Brenninkmeijer, C. A.; Röckmann, T.; Van Der Veen, C.; Tyler, S. C.; Fujita, R.; Morimoto, S.; Aoki, S.; Sowers, T.; Schmitt, J.; et al. Interlaboratory comparison of  $\delta^{13}\text{C}$  and  $\delta\text{D}$  measurements of atmospheric  $\text{CH}_4$  for combined use of data sets from different laboratories. *Atmospheric Measurement Techniques* **2018**, *11*, 1207–1231.
- (32) Thorpe, A.; Frankenberg, C.; Roberts, D. Retrieval techniques for airborne imaging of methane concentrations using high spatial and moderate spectral resolution: application to AVIRIS. *Atmospheric Measurement Techniques* **2014**, *7*, 491–506.
- (33) Thompson, D.; Leifer, I.; Bovensmann, H.; Eastwood, M.; Fladelland, M.; Frankenberg, C.; Gerilowski, K.; Green, R.; Kratwurst, S.; Krings, T.; et al. Real-time remote detection and measurement for airborne imaging spectroscopy: a case study with methane. *Atmospheric Measurement Techniques* **2015**, *8*, 4383–4397.
- (34) Foote, M. D.; Dennison, P. E.; Thorpe, A. K.; Thompson, D. R.; Jongaramrungruang, S.; Frankenberg, C.; Joshi, S. C. Fast and accurate retrieval of methane concentration from imaging spectrometer data using sparsity prior. *IEEE Transactions on Geoscience and Remote Sensing* **2020**, *58*, 6480–6492.
- (35) Guanter, L.; Irakulis-Loitxate, I.; Gorroño, J.; Sánchez-García, E.; Cusworth, D. H.; Varon, D. J.; Cogliati, S.; Colombo, R. Mapping methane point emissions with the PRISMA spaceborne imaging spectrometer. *Remote Sensing of Environment* **2021**, *265*, No. 112671.
- (36) Roger, J.; Guanter, L.; Gorroño, J.; Irakulis-Loitxate, I. Exploiting the entire near-infrared spectral range to improve the detection of methane plumes with high-resolution imaging spectrometers. *Atmospheric Measurement Techniques* **2024**, *17*, 1333–1346.
- (37) Berk, A.; Conforti, P.; Kennett, R.; Perkins, T.; Hawes, F.; Van Den Bosch, J. MODTRAN® 6: A major upgrade of the MODTRAN® radiative transfer code. 2014 6th Workshop on Hyperspectral Image and Signal Processing: Evolution in Remote Sensing (WHISPERS), 2014; pp 1–4.
- (38) Thompson, D.; Thorpe, A.; Frankenberg, C.; Green, R.; Duren, R.; Guanter, L.; Hollstein, A.; Middleton, E.; Ong, L.; Ungar, S. Space-based remote imaging spectroscopy of the Aliso Canyon  $\text{CH}_4$  superemitter. *Geophys. Res. Lett.* **2016**, *43*, 6571–6578.
- (39) Irakulis-Loitxate, I.; Guanter, L.; Liu, Y.-N.; Varon, D. J.; Maasackers, J. D.; Zhang, Y.; Chulakadabba, A.; Wofsy, S. C.; Thorpe, A. K.; Duren, R. M.; et al. Satellite-based survey of extreme methane emissions in the Permian basin. *Sci. Adv.* **2021**, *7*, No. eabf4507.
- (40) Sherwin, E. D.; El Abbadi, S. H.; Burdeau, P. M.; Zhang, Z.; Chen, Z.; Rutherford, J. S.; Chen, Y.; Brandt, A. R. Single-blind test of nine methane-sensing satellite systems from three continents. *Atmospheric Measurement Techniques* **2024**, *17*, 765–782.
- (41) Cusworth, D. H.; Duren, R. M.; Thorpe, A. K.; Tseng, E.; Thompson, D.; Guha, A.; Newman, S.; Foster, K. T.; Miller, C. E. Using remote sensing to detect, validate, and quantify methane emissions from California solid waste operations. *Environmental Research Letters* **2020**, *15*, No. 054012.
- (42) Varon, D. J.; Jacob, D. J.; Jervis, D.; McKeever, J. Quantifying time-averaged methane emissions from individual coal mine vents with GHGSat-D satellite observations. *Environ. Sci. Technol.* **2020**, *54*, 10246–10253.
- (43) Jacob, D. J.; Varon, D. J.; Cusworth, D. H.; Dennison, P. E.; Frankenberg, C.; Gautam, R.; Guanter, L.; Kelley, J.; McKeever, J.; Ott, L. E.; et al. Quantifying methane emissions from the global scale down to point sources using satellite observations of atmospheric methane. *Atmos. Chem. Phys. Discuss.* **2022**, *22*, 9617–9646.
- (44) Chanton, J. P.; Rutkowski, C. M.; Schwartz, C. C.; Ward, D. E.; Boring, L. Factors influencing the stable carbon isotopic signature of methane from combustion and biomass burning. *Journal of Geophysical Research: Atmospheres* **2000**, *105*, 1867–1877.
- (45) Chanton, J. P.; Rutkowski, C. M.; Schwartz, C. C.; Ward, D. E.; Boring, L. Factors influencing the stable carbon isotopic signature of methane from combustion and biomass burning. *Journal of Geophysical Research: Atmospheres* **2000**, *105*, 1867–1877.
- (46) Royer, S. J.; Ferrón, S.; Wilson, S. T.; Karl, D. M. Production of methane and ethylene from plastic in the environment. *PLoS One* **2018**, *13*, No. e0200574.
- (47) Klintzsch, T.; Geisinger, H.; Wieland, A.; Langer, G.; Nehrke, G.; Bizic, M.; Greule, M.; Lenhart, K.; Borsch, C.; Schroll, M.; Keppler, F. Stable Carbon Isotope Signature of Methane Released From Phytoplankton. *Geophys. Res. Lett.* **2023**, *50*, No. e2023GL103317.
- (48) Al-Shalan, A.; Lowry, D.; Fisher, R. E.; Nisbet, E. G.; Zazzeri, G.; Al-Sarawi, M.; France, J. L. Methane emissions in Kuwait: Plume identification, isotopic characterisation and inventory verification. *Atmos. Environ.* **2022**, *268*, No. 118763.
- (49) Douglas, P. M. J.; Stratigopoulos, E.; Park, S.; Phan, D. Geographic variability in freshwater methane hydrogen isotope ratios and its implications for global isotopic source signatures. *Biogeosciences* **2021**, *18*, 3505–3527.
- (50) Brownlow, R.; Lowry, D.; Fisher, R. E.; France, J. L.; Lanoisellé, M.; White, B.; Wooster, M. J.; Zhang, T.; Nisbet, E. G. Isotopic Ratios of Tropical Methane Emissions by Atmospheric Measurement. *Global Biogeochemical Cycles* **2017**, *31*, 1408–1419.
- (51) Cotovicz, L. C.; Abril, G.; Sanders, C. J.; Tait, D. R.; Maher, D. T.; Sippo, J. Z.; Holloway, C.; Yau, Y. Y.; Santos, I. R. Methane oxidation minimizes emissions and offsets to carbon burial in mangroves. *Nature Climate Change* **2024**, *14*, 275–281.
- (52) Tu, Q.; et al. Quantification of  $\text{CH}_4$  emissions from waste disposal sites near the city of Madrid using ground- and space-based observations of COCCON, TROPOMI and IASI. *Atmospheric Chemistry and Physics* **2022**, *22*, 295–317.
- (53) Maasackers, J. D.; Varon, D. J.; Elfarsdóttir, A.; McKeever, J.; Jervis, D.; Mahapatra, G.; Pandey, S.; Lorente, A.; Borsdorff, T.; Foorhuis, L. R.; Schuit, B. J.; Tol, P.; Van Kempen, T. A.; Van Hees, R.; Aben, I. Using satellites to uncover large methane emissions from landfills. *Sci. Adv.* **2022**, *8*, 9683.

(54) Manheim, D. C.; Yeşiller, N.; Hanson, J. L. Gas emissions from municipal solid waste landfills: a comprehensive review and analysis of global data. *Journal of the Indian Institute of Science* **2021**, *101*, 625–657.

(55) Ho, B. Q.; Vu, K. H. N.; Nguyen, T. T.; Nguyen, H. T. T.; Ho, D. M.; Nguyen, H. N.; Nguyen, T. T. T. Study loading capacities of air pollutant emissions for developing countries: a case of Ho Chi Minh City, Vietnam. *Sci. Rep.* **2020**, *10*, 5827.

(56) Palmioto, M.; Fattore, E.; Paiano, V.; Celeste, G.; Colombo, A.; Davoli, E. Influence of a municipal solid waste landfill in the surrounding environment: Toxicological risk and odor nuisance effects. *Environ. Int.* **2014**, *68*, 16–24.

(57) Mattiello, A.; Chiadini, P.; Bianco, E.; Forgione, N.; Flammia, I.; Gallo, C.; Pizzuti, R.; Panico, S. Health effects associated with the disposal of solid waste in landfills and incinerators in populations living in surrounding areas: a systematic review. *International journal of public health* **2013**, *58*, 725–735.

(58) Fang, Y.; Naik, V.; Horowitz, L. W.; Mauzerall, D. L. Air pollution and associated human mortality: The role of air pollutant emissions, climate change and methane concentration increases from the preindustrial period to present. *Atmospheric Chemistry and Physics* **2013**, *13*, 1377–1394.

(59) Mønster, J.; Samuelsson, J.; Kjeldsen, P.; Scheutz, C. Quantification of methane emissions from 15 Danish landfills using the mobile tracer dispersion method. *Waste Manage.* **2015**, *35*, 177–186.

(60) Morris, J.; Matthews, H. S.; Morawski, C. Review and meta-analysis of 82 studies on end-of-life management methods for source separated organics. *Waste Manage.* **2013**, *33*, 545–551.

(61) Powell, J. T.; Townsend, T. G.; Zimmerman, J. B. Estimates of solid waste disposal rates and reduction targets for landfill gas emissions. *Nature Climate Change* **2016**, *6*, 162–165.

(62) Danthurebandara, M.; Van Passel, S.; Nelen, D.; Tielemans, Y.; Van Acker, K. Environmental and socio-economic impacts of landfills. *Linnaeus Eco-Tech* **2012**, *2012*, 40–52.

(63) Clairotte, M.; Suarez-Bertoa, R.; Zardini, A. A.; Giechaskiel, B.; Pavlovic, J.; Valverde, V.; Ciuffo, B.; Astorga, C. Exhaust emission factors of greenhouse gases (GHGs) from European road vehicles. *Environ. Sci. Eur.* **2020**, *32*, 125.

(64) Hopkins, F. M.; Ehleringer, J. R.; Bush, S. E.; Duren, R. M.; Miller, C. E.; Lai, C.-T.; Hsu, Y.-K.; Carranza, V.; Randerson, J. T. Mitigation of methane emissions in cities: How new measurements and partnerships can contribute to emissions reduction strategies. *Earth's Fut.* **2016**, *4*, 408–425.

(65) Dowd, E.; Manning, A. J.; Orth-Lashley, B.; Girard, M.; France, J.; Fisher, R. E.; Lowry, D.; Lanoisellé, M.; Pitt, J. R.; Stanley, K. M. First validation of high-resolution satellite-derived methane emissions from an active gas leak in the UK. *Atmos. Meas. Tech.* **2023**, *17*, 1599–1615.

(66) Woolley Maisch, C. A.; Fisher, R. E.; France, J. L.; Lowry, D.; Lanoisellé, M.; Bell, T. G.; Forster, G.; Manning, A. J.; Michel, S. E.; Ramsden, A. E. Methane Source Attribution in the UK Using Multi-Year Records of CH<sub>4</sub> and δ<sup>13</sup>C. *J. Geophys. Res.: Atmos.* **2023**, *128*, No. e2023JD039098.

(67) Hancock, S. E.; Jacob, D. J.; Chen, Z.; Nesser, H.; Davitt, A.; Varon, D. J.; Sulprizio, M. P.; Balasus, N.; Estrada, L. A.; Cazorla, M.; et al. Satellite quantification of methane emissions from South American countries: a high-resolution inversion of TROPOMI and GOSAT observations. *Atmospheric Chemistry and Physics* **2025**, *25*, 797–817.

#### NOTE ADDED AFTER ASAP PUBLICATION

This paper was published ASAP on November 11, 2025. Author David Orham was added and the paper was reposted on March 3, 2026.



CAS BIOFINDER DISCOVERY PLATFORM™

## PRECISION DATA FOR FASTER DRUG DISCOVERY

CAS BioFinder helps you identify targets, biomarkers, and pathways

Unlock insights

**CAS**  
A division of the American Chemical Society